

# Hypoxia-induced miR-424 decreases tumor sensitivity to chemotherapy by inhibiting apoptosis

D Zhang<sup>1,2</sup>, Z Shi<sup>1</sup>, M Li<sup>\*2</sup> and J Mi<sup>\*1</sup>

**Chemotherapy resistance of tumor cells is a big challenge. Adaptation to hypoxia is an essential cellular response that is controlled by the master oxygen-sensitive transcription factor HIF1 (hypoxia-inducible factor 1). The mechanism by which tumor cells acquire resistance to chemotherapy under hypoxic conditions is not fully understood. In this study, we found that hypoxia induces miR-424 expression and that miR-424 in turn suppresses the level of PDCD4 protein, a tumor suppressor that is involved in apoptosis, by targeting its 3' untranslated region. Functionally, miR-424 overexpression decreases the sensitivity of cancer cells (HCT116 and A375) to doxorubicin (Dox) and etoposide. In contrast, the inhibition of miR-424 enhanced apoptosis and increased the sensitivity of cancer cells to Dox. In a xenograft tumor model, miR-424 overexpression promoted tumor growth following Dox treatment, suggesting that miR-424 promotes tumor cell resistance to Dox. Furthermore, miR-424 levels are inversely correlated with PDCD4 expression in clinical breast cancer samples. These results suggest that miR-424 is a potential molecular target for tumor therapy.**

*Cell Death and Disease* (2014) 5, e1301; doi:10.1038/cddis.2014.240; published online 26 June 2014

Hypoxia is a common feature of rapidly growing tumors. Hypoxic stress induces various physiological or pathophysiological responses in conditions including high-altitude adaptations, development, wound healing, ischemic heart disease, advanced atherosclerosis, stroke, and tumorigenesis.<sup>1</sup> These multifaceted changes are controlled by a panel of hypoxia-inducible genes.<sup>2</sup> Among these genes, hypoxia-inducible factor 1 $\alpha$  (HIF1 $\alpha$ ) is the key transcription factor that is robustly induced by oxygen deprivation; in turn, HIF1 $\alpha$  increases the expression of hundreds of genes that are involved in angiogenesis, cell cycle arrest, and metastasis.<sup>2</sup> Moreover, hypoxia also promotes tumor cell resistance to apoptosis,<sup>3,4</sup> however, the detailed mechanism is not fully understood.

MicroRNAs are evolutionarily conserved, endogenous, non-coding, single-stranded RNAs, 20–23 nucleotides in length, that negatively regulate gene expression in a sequence-specific manner.<sup>5–8</sup> The human genome is predicted to encode as many as 1000 miRNAs, which equates to 3% of the total number of human genes.<sup>7</sup> The 5' portion of the miRNA sequence containing bases two to eight, termed the seed region, is important for target messenger RNA (mRNA) recognition. miRNAs negatively regulate target gene expression through complementarity between the miRNA seed sequence and the 3' untranslated region (UTR) of the target mRNA. miRNAs that bind with perfect complementarity to the protein-encoding mRNA result in the degradation of the target mRNA, whereas miRNAs with imperfect complementarity to

the 3'UTR of the target mRNA will repress mRNA translation. Expression of ~30% of the human proteins appears to be regulated by miRNAs.<sup>9</sup> Through interactions with 3'UTRs, miRNAs can modulate the expression of many genes simultaneously, often regulating individual signaling pathways at multiple levels.<sup>10,11</sup>

Inside a primary tumor, the rapid proliferation of cancer cells frequently outgrows its blood supply, leaving many tumor cells in regions where the oxygen concentration is significantly lower than the normal tissues.<sup>12</sup> To survive in the hypoxic microenvironment, cancer cells have altered their intrinsic gene expression patterns to inhibit apoptosis. Recent studies have demonstrated that hypoxia induces the expression of a number of miRNAs, termed 'hypoxamirs', and these miRNAs coordinate HIF signaling to regulate cell growth, apoptosis, and metastasis.<sup>13</sup> For example, the elevated expression of miR-210 under hypoxic conditions in breast cancer, melanoma, pancreatic cancer, and ovarian cancer has been reported to correlate with cell growth and metastasis by suppressing the expression of MYC, the cell cycle regulator E2F transcription factor 3, the receptor tyrosine kinase ligand ephrin A3, and the DNA repair protein RAD52.<sup>14–16</sup> miR-424 is also induced by hypoxia in endothelial cells, leading to the suppression of the scaffolding protein cullin 2 (CUL2), which is critical for the assembly of the ubiquitin ligase system, resulting in the stabilization of HIF1 $\alpha$  and the promotion of angiogenesis.<sup>17</sup> However, whether

<sup>1</sup>Department of Biochemistry & Molecular Cell Biology, Shanghai Key Laboratory of Tumor Microenvironment and Inflammation, Shanghai Jiao Tong University School of Medicine, Shanghai, China and <sup>2</sup>Institute of Cancer Stem Cell, Dalian Medical University, Dalian, China

\*Corresponding authors: M Li, Institute of Cancer Stem Cell, Dalian Medical University, Dalian 116044, China. Tel: +86 411 86110293; Fax: +86 411 86110012; E-mail: molin\_li@hotmail.com

or J Mi, Institute of Medical Science, Shanghai Jiao Tong University School of Medicine; 280 South Chongqing Road, Shanghai 200025, China. Tel: +86 21 63846590 + 776491; Fax: +86 21 54660873; E-mail: jmei@sjtu.edu.cn

**Abbreviations:** PDCD4, programmed cell death 4; HIF1, hypoxia-inducible factor 1; Dox, doxorubicin; 3'UTR, 3' untranslated region; MYC, v-myc avian myelocytomatosis viral oncogene homolog; CUL2, cullin 2; DMOG, dimethylxaloylglycine; PHD, prolyl hydroxylase domain; HRE, hypoxia response element; ChIP, chromatin immunoprecipitation; shRNA, short hairpin RNA; PARP, poly ADP ribose polymerase; PCR, polymerase chain reaction; TUNEL, terminal deoxynucleotidyl transferase dUTP nick end labeling; RNU48, small nucleolar RNA, C/D box 48; PBS, phosphate-buffered saline; CKK8, Cell Counting Kit-8

Received 31.12.13; revised 29.3.14; accepted 11.4.14; Edited by E Candi

miR-424 is increased and regulates apoptosis in the tumor is unclear.

In this study, we demonstrated that the level of miR-424 increases in cancer cells and promotes chemotherapy resistance in tumor cells, suggesting that miR-424 is a potential molecular target for sensitizing treatment.

## Results

**Hypoxia induces the expression of miR-424 in tumor cells.** Previous studies have shown that hypoxia induces miR-424 expression in endothelial cells, but whether hypoxia regulates miR-424 expression in tumor cells had not been elucidated. The microRNA profiling by deep sequencing showed that the expression of miR-424 increased in human melanoma A375 cells after 6 h in 1% oxygen (Figure 1a).

To select tumor cells that upregulate miR-424 under hypoxia, melanoma A375 cells, glioblastoma U251 cells, and colon cancer HCT116 cells were grown for 12 h in 1% oxygen or were treated with H<sub>2</sub>O<sub>2</sub> or DMOG, a prolyl hydroxylase domain (PHD) enzyme inhibitor. Both DMOG and H<sub>2</sub>O<sub>2</sub> are well-established reagents that induce the accumulation of HIF1- $\alpha$ . The mature miR-424 and pri-miR-424 were measured using quantitative PCR in these cells. The data show that the levels of both the mature miR-424 and pri-miR-424 increased in all three cell lines under hypoxic conditions and were ~2–3-fold higher than normoxic cells (Figures 1b and c). Moreover, the levels of both mature miR-424 and pri-miR-424 also increased in the three tumor cell lines treated with DMOG or H<sub>2</sub>O<sub>2</sub> (Figures 1b and c), which accumulated the protein level of HIF1 $\alpha$  in these cells, as evaluated by western blot analysis (Figure 1d). As expected, the knockdown of HIF1 $\alpha$  decreased the expression of miR-424 (Supplementary Figure S1A). These observations suggest that HIF1 $\alpha$  is involved in the regulation of miR-424 expression.

To identify whether HIF1 $\alpha$  regulates miR-424 expression, conserved HIF1 $\alpha$ -binding sequences GCGTG (hypoxia response element, HRE) accompanied by CACA were found in the ~2.5 kb pairs upstream of pri-miR-424 (Figure 1e). To investigate whether HIF1 $\alpha$  binds to the promoter of the miR-424 gene, chromatin immunoprecipitation (ChIP) assays were performed. Our data showed that HIF1 $\alpha$  binds to HRE elements in the 2.5 kb upstream of the miR-424 promoter, suggesting that HIF1 $\alpha$  regulates miR-424 expression. Although Ghosh *et al.*<sup>17</sup> showed that miR-424 expression in endothelial cells is induced by hypoxia at the transcriptional level via PU.1 transactivation, our data demonstrated that HIF1 $\alpha$  regulates miR-424 expression in tumor cells, at least in these three tumor cell lines; nevertheless, we cannot exclude the possibility that PU.1 also regulates miR-424 expression.

To further confirm whether the putative HRE in the miR-424 promoter is functional, a 1000-bp fragment encompassing the miR-424 promoter HRE was inserted into pGL3 promoter. 293T cells transfected with wild-type miR-424 promoter reporter, control reporter, mutant miR-424 promoter, and pSV-Renilla vector were exposed to 20% O<sub>2</sub> or 1% O<sub>2</sub> for 12 h. The wild type of miR-424 promoter significantly increased FLuc activity in hypoxia cells (Figure 1f). The mutation of HRE at the core binding site, eliminating HIF1 $\alpha$

binding, significantly decreased hypoxia-induced Fluc activity. Knockdown of HIF1 $\alpha$  using short hairpin RNAs (shRNAs) significantly reduced miR-424 promoter HRE-dependent Fluc activity in hypoxic cells (Supplementary Figure S1B). Taken together, these data demonstrated that HIF1 $\alpha$  binds to the HRE site in the miR-424 promoter and directly activates its transcription.

## miR-424 increases tumor cell resistance to apoptosis.

To explore the biological significance of miR-424 in tumors, doxorubicin (Dox)-induced apoptosis was first analyzed in the A375 and HCT116 cells, as both of these cell lines overexpress miR-424. The tumor cells infected with empty lentivirus were used as a control. Western blot analysis showed that Dox dramatically induced the cleavage of caspase-3 and PARP, both of which are markers of apoptosis; overexpression of miR-424 attenuated the level of cleaved caspase-3 and PARP, suggesting that miR-424 inhibits the Dox-induced apoptosis (Figures 2a and b). Moreover, etoposide-induced apoptosis was also analyzed in the A375 and HCT116 cells transfected with miR-424 mimics; the transfection efficiency was assessed by quantitative PCR (Supplementary Figure S2A). Flow cytometry analysis showed that etoposide significantly induced the turnover of annexin V, another marker of apoptosis; overexpression of miR-424 minimized the percentage of annexin V-positive cells in both cell lines, suggesting that miR-424 overexpression suppresses etoposide-induced apoptosis (Figures 2c and d).

To further confirm the effects of miR-424 on apoptosis in tumor cells, Dox-induced apoptosis was analyzed in A375 and HCT116 cells transfected with the miR-424 inhibitor (anti-sense oligomer), and the tumor cells transfected with non-specific oligos were used as a control. The transfection efficiency was detected by quantitative PCR (Supplementary Figure S2B). Western blot analysis showed that Dox treatment resulted in the cleavage of caspase-3 and PARP; the miR-424 inhibitor enhanced the levels of cleaved caspase-3 and PARP (Figure 2e). Furthermore, etoposide-induced apoptosis was also analyzed in the A375 and HCT116 cells transfected with the miR-424 inhibitor. Flow cytometry analysis showed that etoposide significantly induced the turnover of annexin V; transfection of the miR-424 inhibitor increased the percentage of annexin V-positive cells in both cell lines (Figures 2f and g). These observations suggest that miR-424 inhibits Dox-induced apoptosis, and both Dox and etoposide themselves did not affect the expression of miR-424 (Supplementary Figures S2C and D). Finally, the survival ratio of HCT116 cells treated with 10 nM Dox was determined using the CCK8 assay, and the data show that overexpression of miR-424 improved the survival of HCT116 cells. The survival ratio increased from 30.9 to 54.5% on the third day (Figure 2h), suggesting that miR-424 increased the number of HCT116 cells resistant to Dox.

Briefly, these observations suggested that overexpression of miR-424 protects the tumor cells from apoptosis and increases tumor cell resistance to therapeutic chemicals.

## miR-424 suppresses the expression of PDCD4, a tumor suppressor involved in apoptosis.

To dissect the

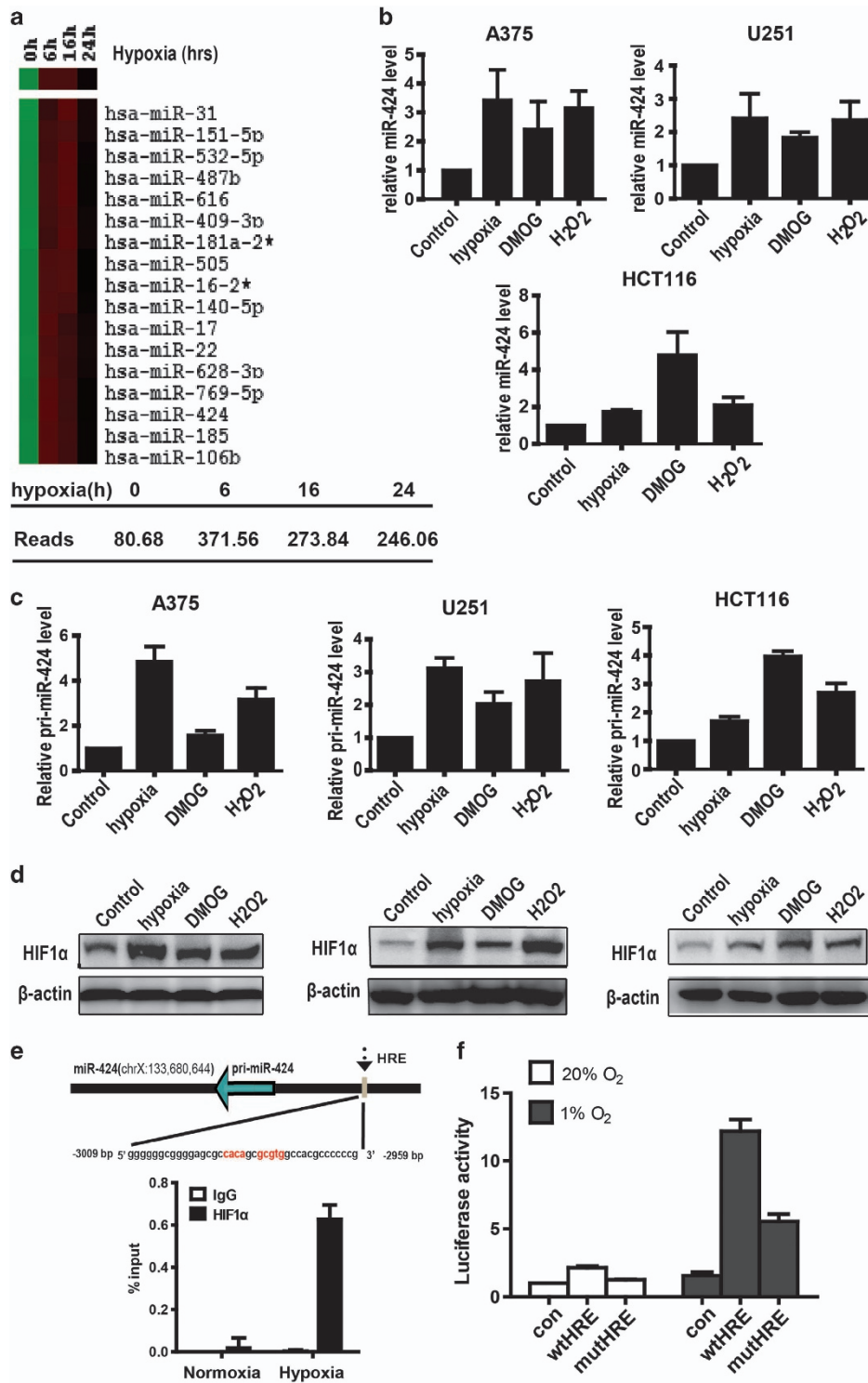


**Figure 1** Hypoxia increases miR-424 expression in cancer cells. **(a)** Hypoxia increases miR-424 expression in melanoma A375 cells. A selected heatmap of microRNA profiling, which was analyzed by deep sequencing in melanoma A375 cells, is shown for different time points under hypoxic conditions. The color from green to dark red indicated the expression level of miRNAs, from low to high. **(b)** Hypoxia increases the level of mature miR-424 in different cancer cell lines. The level of miR-424 was individually analyzed using quantitative PCR analysis in A375, U251, and HCT116 cells, which were treated with 1% O<sub>2</sub>, 2 mM DMOG, or 40 μM H<sub>2</sub>O<sub>2</sub>. **(c)** Hypoxia increases miR-424 expression in different cancer cell lines. The level of pri-miR-424 was analyzed using quantitative PCR in the A375, U251, and HCT116 cancer cell lines treated as above. **(d)** The protein level of HIF1α increased under hypoxia. The A375, HCT116, and U251 cells were treated with 1% O<sub>2</sub>, 2 mM DMOG, or 40 μM H<sub>2</sub>O<sub>2</sub>; the protein level of HIF1α was evaluated by western blot analysis. **(e)** HIF1α specifically binds the putative HRE site in the promoter of miR-424. Chromatin IP was performed in hypoxia-induced A375 cells (12 h) using antibody against HIF1α, or IgG, and analyzed by qPCR. MiR-424 occupancy by HIF1α was significantly enriched compared to IgG. **(f)** 293T cells were cotransfected with pGL3p control, pGL3p-wt miR-424 HRE (HRE wt), or pGL3p-mutant miR-424 HRE (HRE mut) and pSV-Renilla and were exposed to 20% or 1% O<sub>2</sub> for 12 h. The ratio of Fluc:Rluc activity was normalized to control at 20% O<sub>2</sub>. The miR-424 HRE significantly increased Fluc activity in hypoxic condition

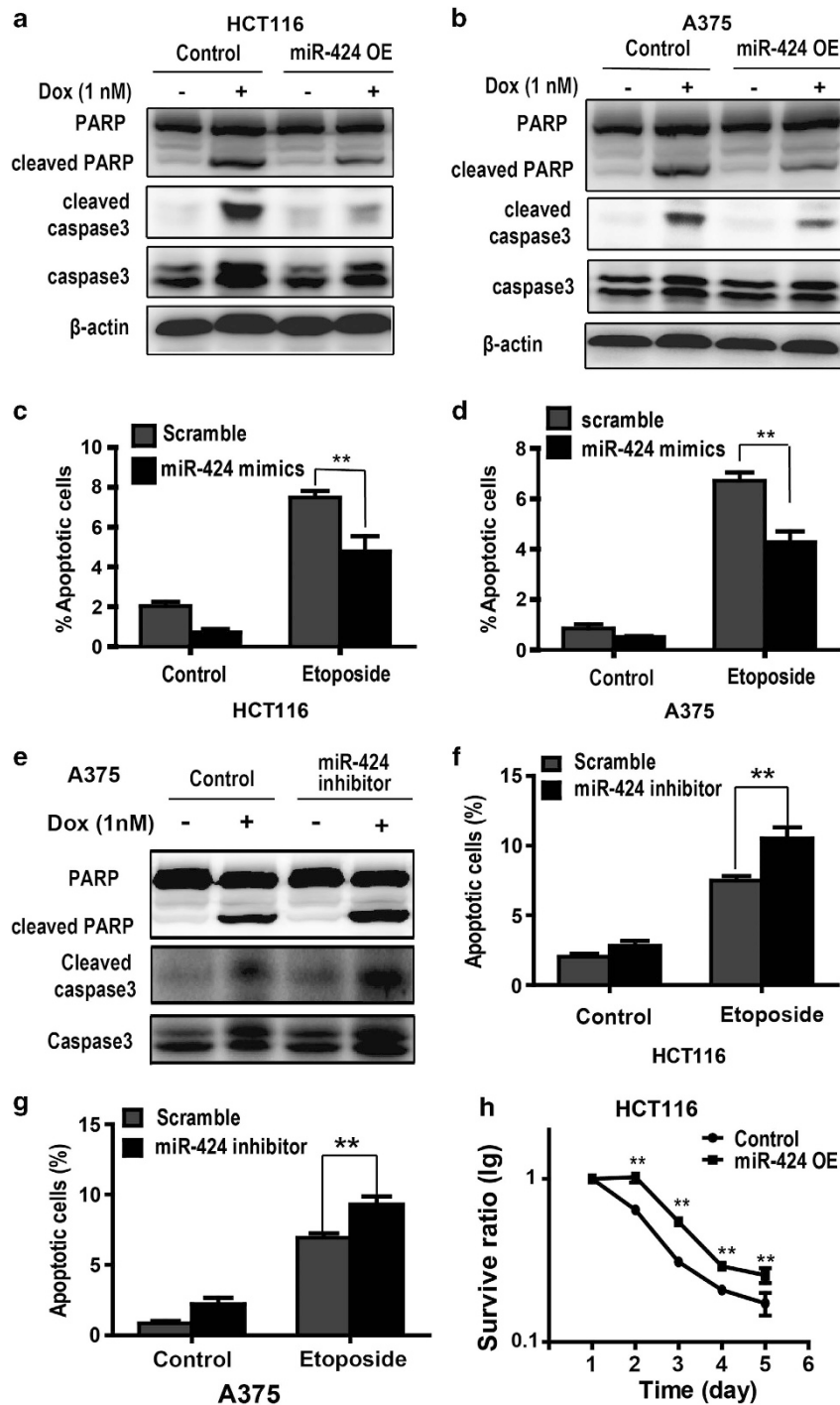


**Figure 2** The overexpression of miR-424 suppresses the apoptosis of tumor cells induced by anti-cancer chemicals. (a and b) Cleaved PARP and cleaved caspase-3 were detected using western blot analysis in HCT116 and A375 cells, which were transfected with a scrambled oligo or a miRNA-424 mimic. The final concentration of doxorubicin was 1 nM. (c and d) The annexin V-positive population of HCT116 or A375 cells was analyzed using flow cytometry. The final concentration of etoposide was 100  $\mu$ M or 5  $\mu$ M. (e) Cleaved PARP and cleaved caspase-3 levels were detected using western blot analysis in A375 cells that were transfected with a scrambled oligo or the miRNA-424 inhibitor. (f and g) The annexin V-positive populations of HCT116 or A375 cells were analyzed using flow cytometry. The final concentration of etoposide was 100  $\mu$ M and 5  $\mu$ M, respectively. (h) The survival ratio was analyzed using the CCK8 assay in HCT116 cells treated with doxorubicin (10 nM). HCT116 cells were transfected with the miRNA-424 mimic or inhibitor

mechanism by which miR-424 increases tumor cell resistance to therapeutic chemicals, the downstream effectors of miR-424 were identified using the web-based software TargetScan. PDCD4, PDCD11, PDCD6IP, and DEDD are

apoptosis-related proteins that are potentially targeted by miR-424 based on pairing of the seed sequence of miR-424 (Figure 3a). The 3'UTR of these candidates was cloned into a dual-luciferase UTR vector, as shown in the schematic



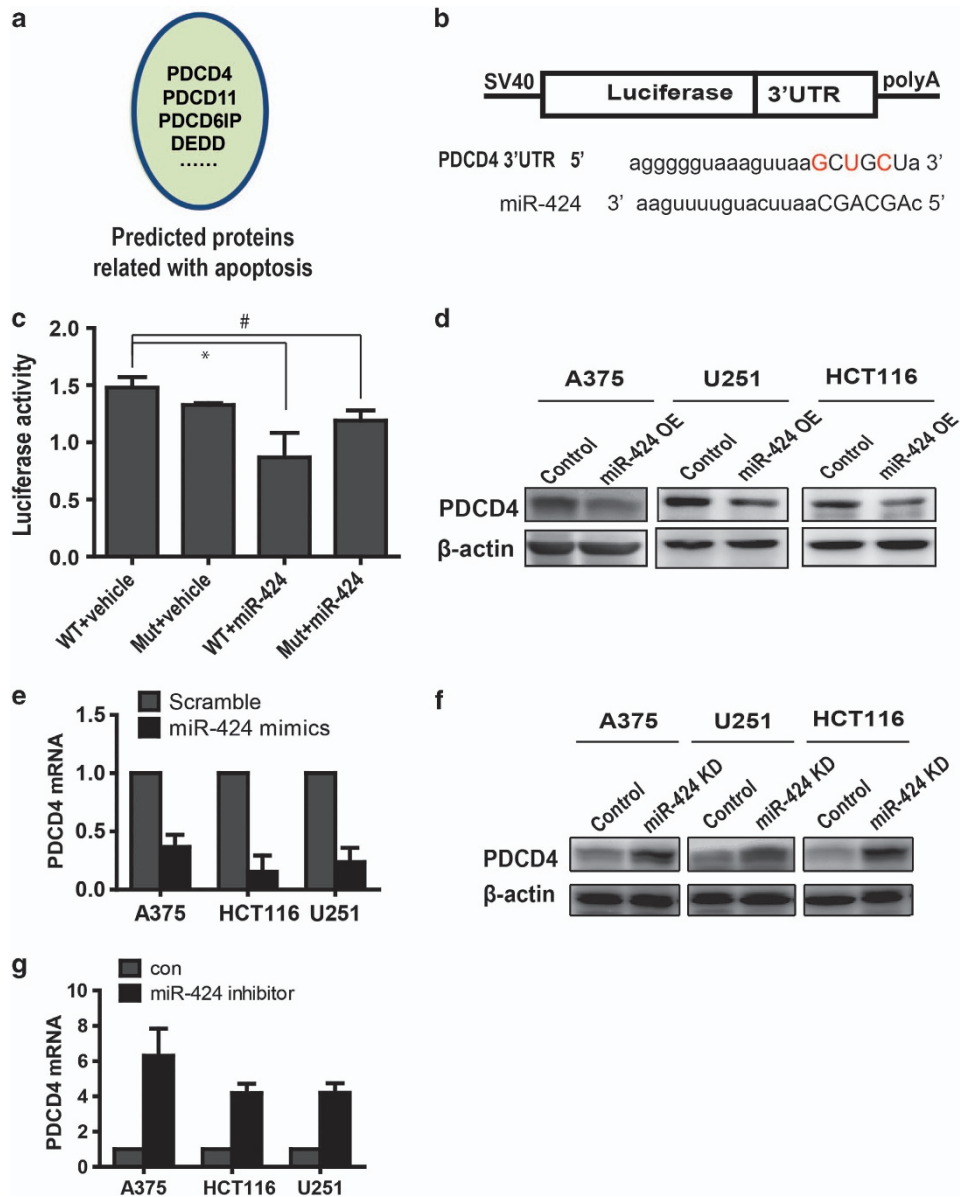


**Figure 3** miR-424 regulates PDCD4 expression. (a) Proteins regulating apoptosis were predicted to be targets of miR-424. (b) This sequence in the 3'UTR of PDCD4 was predicted to bind to miR-424. The nucleotides in red were mutated to their complementary nucleotides. (c) 3'UTR luciferase assay showing the repression of wild-type UTR or mutant UTR following transfection of the miR-424 mimic or scrambled miRNA ( $*P < 0.05$ ;  $\#P > 0.05$ ). (d) miR-424 overexpression inhibits the protein level of PDCD4 in A375 and fibroblast cells, which were evaluated using western blot analysis. (e) miR-424 knockdown increased the protein level of PDCD4 in A375, U251, and HCT116 cells. (f) The miR-424 mimic inhibited the mRNA level of PDCD4 in A375 and HCT116, as analyzed by quantitative PCR. (g) The miR-424 inhibitor increased the mRNA level of PDCD4 in A375 and HCT116 cells

(Figure 3b), and the 3'UTR luciferase assay was performed. However, the luciferase activity was only significantly reduced by miR-424 in the cells expressing the wild-type PDCD4 3'UTR (Figure 3c), but not in the cells expressing the 3'UTRs of PDCD11, PDCD6IP, or DEDD (data not shown). The capital letters indicate the potential binding sequence of miR-424; when the three nucleotides indicated in red were mutated into their complementary nucleotides, miR-424 could no longer affect the luciferase activity.

Therefore, the protein level of PDCD4 was further determined using western blot analysis in A375, HCT116, and U251 cells and fibroblasts overexpressing miR-424. The

data showed that overexpression of miR-424 dramatically decreased the PDCD4 protein level (Figure 3d). Moreover, the mRNA level of PDCD4 was also analyzed using quantitative PCR in A375, HCT116, and U251 cells transfected with the miR-424 mimic oligos. As the graph shows, the miR-424 mimics reduced the PDCD4 mRNA level to 40%, 15%, or 25% in the A375, HCT116, or U251 cells, respectively (Figure 3e). In contrast, miR-424 knockdown increased the PDCD4 protein level in A375, U251, and HCT116 cells (Figure 3f), and the mRNA level of PDCD4 increased sixfold in A375, HCT116, or U251 cells transfected with the miR-424 inhibitor (Figure 3g), compared to the control A375 cells.

**miR-424 increases tumor resistance to therapeutic chemicals *in vivo*.** To evaluate the impact of miR-424 on tumor resistance to therapeutic drugs, Balb/c nude mice were used for the xenograft tumor model. The control A375 cells or A375 cells overexpressing miR-424 were subcutaneously injected into the bilateral armpits of nude mice. Dox (2 mg/ml) was administered in the drinking water 7 days after injection, and the volumes of the xenograft tumors were measured after sacrifice at the 15th day post inoculation. As shown in Figure 4a, Dox treatment dramatically inhibited tumor growth in both the miR-424 overexpression group and control group, but there was a significant increase in tumor size in the miR-424 overexpression group as compared with

the control group. However, without Dox treatment, there was no significant difference in tumor size between the miR-424 group and control group. Moreover, with Dox treatment, the tumor also grew faster in the miR-424 overexpression group than the control group (Figure 4b), suggesting that miR-424 increased tumor resistance to Dox treatment.

*In situ* TUNEL analysis on cryogenic sections from xenograft tumor showed that the tumors overexpressing miR-424 had less TUNEL-positive cells than the control group, 4.5% *versus* 11% (Figure 4c). Western blots analysis on the xenograft tumor showed that miR-424 decreased the protein level of PDCD4, whose knockdown reduced the level of cleaved PARP (Supplementary Figure S3). However, Dox

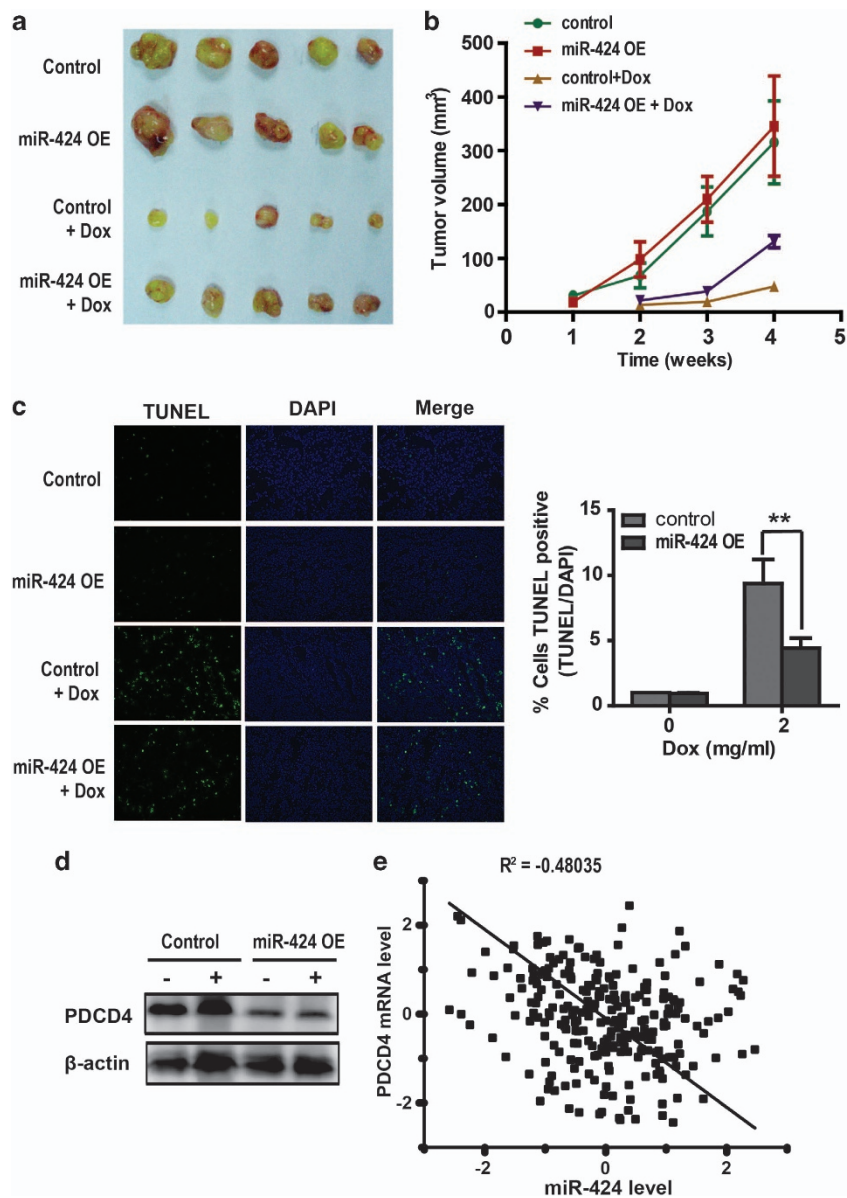


**Figure 4** miR-424 decreases the sensitivity of tumor cells to doxorubicin *in vivo*. (a) Dox (2 mg/ml) was administered to xenograft mice in the drinking water. The photo is a representative image of the xenograft tumors. (b) The tumor growth rate were analyzed between the four groups. (c) The TUNEL-positive cells were analyzed in the tumor sections (original magnification, 20 ×); the percentage of TUNEL-positive cells in this four groups was quantified. (d) Dox treatment did not change PDCD4 expression. The expression of PDCD4 in xenograft tumors was analyzed by western blot. (e) Correlation analysis of miR-424 and PDCD4 expression in clinical breast cancer samples using the Pearson correlation ( $R = -0.48035$ ,  $P < 0.01$ ,  $n = 257$ )

itself had no effect on PDCD4 expression in tumors (Figure 4c and Supplementary Figures S2C and D). These results are consistent with our *in vitro* data that showed that miR-424 regulates apoptosis by targeting PDCD4.

Finally, we performed a comprehensive analysis of miR-424 expression and PDCD4 expression in clinical breast cancer samples, which were obtained from a previously published data set (Gene expression omnibus accession GSE19783) comprising matched mRNA and miRNA expression. This analysis showed that miR-424 expression had a strong inverse correlation with PDCD4 expression in the clinical samples (Figure 4e).

Briefly, these observations suggest that the hypoxia-induced miR-424 promotes tumor resistance to apoptosis, which may result in tumor cell resistance to therapeutic drugs under hypoxic conditions, suggesting that miR-424 level could link to poor prognosis, which was consistent with the data from the Berghmans group.<sup>18</sup>

## Discussion

The resistance of cancer cells to chemotherapy remains a major obstacle for the successful treatment of cancer patients. Multiple mechanisms, including both intracellular and extracellular causes, contribute to chemotherapy resistance. Gene mutations or gene amplifications in tumor cells that influence the uptake, metabolism, or export of drugs were considered the main reasons for chemotherapy resistance. Additionally, recent studies have shown that the specific microenvironment of solid tumors, including the hypoxic conditions and the acidic microenvironment, also increases drug efflux and alters drug metabolism in tumor cells through epigenetic regulation, which might play an important role in chemotherapy resistance. Thus, determining how hypoxic conditions or acidic microenvironments regulate tumor cell chemotherapy resistance is a promising approach for tumor treatment.

Our data and the data from other groups have demonstrated that hypoxia induces the expression of miR-424 in several cell lines. The increased miR-424 expression then targets different downstream genes to regulate cellular functions, including CUL2, which is a scaffolding protein critical for the assembly of the ubiquitin ligase system. The Ramakrishnan group has shown that miR-424 stabilizes HIF1 $\alpha$  and promotes angiogenesis in endothelial cells by targeting CUL2.<sup>17</sup> Our data demonstrated that the hypoxia-induced miR-424 enhanced tumor cell resistance to apoptosis by targeting PDCD4, and A375 cells overexpressing miR-424 were more resistant to Dox treatment in the xenograft tumor model, as compared to the control cells; together, these data suggest that hypoxia increased the tumor cell resistance to chemotherapy and that miR-424 mediates this regulation. These observations suggest that miR-424 might be a molecular target for chemotherapy sensitization.

Additionally, the transcription factor PU.1 was reported to regulate miR-424 expression in endothelial cells. Nevertheless, we also found that HIF1 $\alpha$  increases miR-424 expression. The PHD enzyme inhibitor DMOG, as well as H<sub>2</sub>O<sub>2</sub> and hypoxia, increase miR-424 expression in fibroblast and tumor cells, suggesting that HIF1 $\alpha$  also regulates miR-424 expression. The conserved HIF1 $\alpha$  binding sequences

'GCGTG' are located ~2.5 kb upstream of the pri-miR-424 sequence and inside the sequence of pri-miR-424. Chromatin immunoprecipitation assays further confirmed that HIF1 $\alpha$  regulates the expression of miR-424.

Briefly, our data demonstrated that hypoxia-induced miR-424 expression increases the resistance of tumor cells to apoptosis, resulting in chemotherapy resistance. Therefore, miR-424 is a potential molecular target for tumor therapy.

## Materials and Methods

**Cell culture and reagents.** The A375, U251, HCT116, and HEK293T cancer cell lines were obtained from ATCC (Manassas, VA, USA). Human fibroblasts were isolated from skin foreskin. All cell lines were cultured in DMEM supplemented with 10% heat-inactivated fetal bovine serum (FBS). SYBR Green PCR master mix and TaqMan microRNA reverse transcription kit were purchased from ABI (Foster City, CA, USA). Antibodies against PDCD4, PARP, and cleaved caspase-3 were purchased from Cell Signaling Technology (Boston, MA, USA). The Dual-Luciferase Reporter Assay kit was purchased from Promega (Madison, WI, USA). Etoposide, DMOG, and Dox were obtained from Sigma (St Louis, MO, USA).

**Vector construction.** To construct the pmirGLO-PDCD4-3'UTR-WT plasmid, a fragment of the wild-type 3'UTR of human PDCD4 mRNA (GenBank accession number: NM\_014456.4) containing the putative miR-424 binding sequences (377–398) was amplified and cloned into the *SacI* and *XhoI* sites downstream of the luciferase reporter gene in the pmirGLO-control vector (Promega). pmirGLO-PDCD4-3'UTR-MUT, which carried mutations in the sequence complementary to the seed region of miR-424, was generated based on the pmirGLO-PDCD4-3'UTR-WT plasmid by site-specific mutagenesis using the following primers: forward primer: 5'-AAGTTAACAGGTAAAACCCCATGTTGGTCCAGGT-3'; reverse primer: 5'-ACCTGGACCCAACATGGGGTT-3'.

To construct the miR-424 overexpression vector, two oligonucleotides were synthesized (forward primer: 5'-TCGACAGCAGCAATTCATGTTTTGAAGTGTGCTGTCTTCAAAAACATGAATTGCTGCTGTTTTT-3'; reverse primer: 5'-AATTA AAAA CAGCAGCAATTCATGTTTTGAAGGACAGCACACCTCAAACATGAATTGCTGCTG-3') and were cloned into the *EcoRI* and *XhoI* sites in the pGIPZ vector (OpenBiosystem, Pittsburgh, PA, USA) after annealing.

To construct the pGL3-wtHRE, a fragment of the wild-type HRE from miR-424 promoter was amplified using the following primers: F: 5'-TTTACGCGTTCTCGGTGTTGGTACTCTG-3'; R: 5'-TTTCTCGAGGTCACCTCAGGAGAGGGTCA-3' and cloned into the *MluI* and *XhoI* sites upstream of the luciferase reporter gene in the pGL3-control vector (Promega). pGL3-mutHRE, which carried mutations in the HRE, was generated based on the pGL3-wtHRE plasmid by site-specific mutagenesis using the following primers: F: 5'-GAGCGCGTGTGCCGCACGCCACGCCCCCG-3'; R: 5'-CGGGGGCGGTGCGGTGCGGCACACGCGCTC-3'.

**Transfections.** All transfections were performed using Lipofectamine 2000 (Invitrogen, Carlsbad, CA, USA) according to the manufacturer's instructions. The miR-424 inhibitor, negative controls, and miR-424 mimics were purchased from GenePharm (Shanghai, China). The miRNA inhibitor and mimics were used at a final concentration of 50 nM.

**Luciferase reporter assay.** For the luciferase reporter assay, 293T cells were seeded in a 24-well plate and were grown to 80–90% confluence. To detect the interaction between miR-424 and PDCD4 3'UTR, the cells were then cotransfected with 800 ng of either pGIPZ or pGIPZ-miR-424 and 40 ng of either pmirGLO-PDCD4-3'UTR-WT or pmirGLO-PDCD4-3'UTR-MUT using Lipofectamine 2000 (Invitrogen) according to the manufacturer's protocol. To detect whether the putative HRE in the miR-424 promoter is functional, the cells were collected 48 h after co-transfection and analyzed using the Dual-Luciferase Reporter Assay System (Promega). Luciferase activity was detected using a M200 microplate fluorescence reader. A plasmid constitutively expressing *Renilla* luciferase was cotransfected as an internal control to correct for differences in both the transfection and harvesting efficiencies. The transfections were performed in duplicate, and at least three independent experiments were performed.

**RNA extraction and real-time PCR.** The culture medium was removed, and the cells were immediately washed with ice-cold PBS. Subsequently, 1 ml of TRIzol reagent was added, and total cellular RNA was extracted using the acid



guanidium thiocyanate–phenol–chloroform method. Total RNA (1  $\mu$ g) was used as a template for MMLV-RT reverse transcriptase reaction, which was performed according to the manufacturer's instructions. Real-time quantitative reactions were set up in triplicate in a 96-well plate; each reaction contained 1  $\mu$ l of cDNA and the SYBR Green PCR mix to which gene-specific forward and reverse PCR primers were added.  $\beta$ -Actin was used to normalize the expression of the target genes. Melting curves were analyzed to verify the specificity of the RT-PCR reaction and the absence of primer dimer formation. For the quantitation of miRNAs, the TaqMan MicroRNA reverse transcription kit was used according to the manufacturer's instructions with the stem loop primer, and the results were normalized to RNU48.

**Protein extraction and western blot analysis.** The cells were placed on ice immediately and washed with ice-cold PBS. Total protein extract was prepared using RIPA lysis buffer containing 1  $\times$  protease inhibitor mixture (Roche, Basel, CH, Switzerland) and 1  $\times$  PMSF. The proteins were resolved on 8–12% SDS-polyacrylamide gels and were transferred by electroblotting to nitrocellulose membranes (Bio-Rad, Hercules, CA, USA). The membranes were blocked with 5% nonfat dry milk in TBST for 1 h and incubated overnight at 4  $^{\circ}$ C in 5% BSA in TBS with an anti-PDCD4, anti-PARP, or anti-cleaved caspase-3 antibody. Immunolabeling was detected using the ECL reagent (Sigma).  $\beta$ -Actin expression levels were used as a loading control.

**Lentiviral production and transduction.** HEK 293T cells were seeded in 60 mm plates ( $4 \times 10^6$  cells/plate) in DMEM supplemented with 10% heat-inactivated FBS 1 day prior to transfection. The cells were transfected with 5.2  $\mu$ g of the miR-424 overexpression vector, along with 2.36  $\mu$ g of psPAX2 and 0.8  $\mu$ g of pMD2G using Lipofectamine 2000 in DMEM. After 6 h, the transfection media were removed and replaced with DMEM containing 10% heat-inactivated FBS without penicillin–streptomycin. Lentiviral particles were harvested 72 h post transfection. The melanoma A375 cells were plated in DMEM with 10% FBS at 20% confluence 1 day prior to transduction. The A375 cells were seeded in 60 mm plates and were transduced in 3 ml of additional media containing the viral particles, along with 6  $\mu$ g/ml polybrene. After 16 h, the conditional media were removed and replaced with DMEM supplemented with 10% FBS.

**Cell viability assays.** Cells (5000 cells/well) were seeded into a 96-well plate and treated with Dox. After incubation for 24, 48, 72, or 96 h, the cells were labeled with CKK8 (Dojindo, Tabaru, Japan) for 2 h. Cell viability was measured at an absorbance of 450 nm.

**ChIP assays.** A375 cells cultured in 20% O<sub>2</sub> or 1% O<sub>2</sub> were fixed in 1% formaldehyde for 20 min at 37  $^{\circ}$ C and quenched in 0.125 M glycine. Chromatin was immunoprecipitated with HIF1- $\alpha$  antibody or IgG against sonicated cell lysates and quantified using SYBR Green Real-time PCR analysis. Fold enrichment was calculated based on Ct as  $2^{-\Delta(\Delta Ct)}$ , where  $\Delta Ct = \Delta Ct_{IP} - \Delta Ct_{input}$  and  $\Delta(\Delta Ct) = \Delta Ct_{antibody} - \Delta Ct_{IgG}$ . Primer sequences were as follows: miR-424-F: 5'-GCAGCGGGCCAAGGCTGCGG-3'; miR-424-R: 5'-AACGCTCCCTTGAGGGC-GAG-3'.

**TUNEL analysis.** OCT-embedded sections of tumors were fixed with 4% paraformaldehyde. After permeabilization with 0.1% Triton X-100 in PBS for 10 min, slides were incubated with methanol containing 3% H<sub>2</sub>O<sub>2</sub>, followed by dUTP nick end labeling at 37  $^{\circ}$ C for 1 h.

**Apoptosis assay.** Apoptosis was assessed used Annexin-V-PI. At the ending of the incubation period, floating as well as adherent cells were harvested by trypsinization and washed with PBS. Cells were stained with 5  $\mu$ l annexin V in 60  $\mu$ l 1  $\times$  binding buffer for 15 min at room temperature in dark. After staining, to the cell suspension was added 120  $\mu$ l 1  $\times$  binding buffer and 5  $\mu$ l propidium iodide and analyzed using FACS Calibur flow cytometer (BD, Franklin Lakes, NJ, USA).

**Xenograft tumor model.** A375 cells ( $1 \times 10^6$  cells) stably expressing miR-424 or the vector control were inoculated bilaterally into the armpit region of 3–4 week-old immunodeficient nude mice. Dox (2 mg/ml) was administered in the drinking water 7 days after injection. The tumors weight were measured 15 days after inoculation.

**Statistical analysis.** The data are presented as the mean  $\pm$  S.D. The samples were analyzed using a two-tailed unpaired Student's *t*-test, unless otherwise noted, and *P*-values <0.05 were considered statistically significant. *P*-values <0.05, <0.01, and <0.001 are indicated with one, two, and three asterisks, respectively.

### Conflict of Interest

The authors declare no conflict of interest.

**Acknowledgements.** This study was supported by grants from the National Program on Key Basic Research Project (973 Program) (2012CB910102) (2012CB967000), the Shanghai Committee of Science and Technology (11DZ2260200), and the National Science Foundation of China (81372194) to Dr Mi.

- Chen Z, Lai TC, Jan YH, Lin FM, Wang WC, Xiao H *et al*. Hypoxia-responsive miRNAs target argonaute 1 to promote angiogenesis. *J Clin Invest* 2013; **123**: 1057–1067.
- Vaupel P. The role of hypoxia-induced factors in tumor progression. *Oncologist* 2004; **9**(Suppl 5): 10–17.
- Hockel M, Vaupel P. Tumor hypoxia: definitions and current clinical, biologic, and molecular aspects. *J Natl Cancer Inst* 2001; **93**: 266–276.
- Teicher BA. Hypoxia and drug resistance. *Cancer Metastasis Rev* 1994; **13**: 139–168.
- Bunting SF, Callen E, Wong N, Chen HT, Polato F, Gunn A *et al*. 53BP1 inhibits homologous recombination in Brca1-deficient cells by blocking resection of DNA breaks. *Cell* 2010; **141**: 243–254.
- Cho WC. OncomiRs: the discovery and progress of microRNAs in cancers. *Mol Cancer* 2007; **6**: 60.
- Esquela-Kerscher A, Slack FJ. Oncomirs - microRNAs with a role in cancer. *Nat Rev Cancer* 2006; **6**: 259–269.
- Voorhoeve PM, Agami R. Classifying microRNAs in cancer: the good, the bad and the ugly. *Biochim Biophys Acta* 2007; **1775**: 274–282.
- Lewis BP, Burge CB, Bartel DP. Conserved seed pairing, often flanked by adenosines, indicates that thousands of human genes are microRNA targets. *Cell* 2005; **120**: 15–20.
- Baek D, Villen J, Shin C, Camargo FD, Gygi SP, Bartel DP. The impact of microRNAs on protein output. *Nature* 2008; **455**: 64–71.
- Selbach M, Schwanhauser B, Thierfelder N, Fang Z, Khanin R, Rajewsky N. Widespread changes in protein synthesis induced by microRNAs. *Nature* 2008; **455**: 58–63.
- Brown JM. Tumor hypoxia in cancer therapy. *Meth Enzymol* 2007; **435**: 297–321.
- Loscalzo J. The cellular response to hypoxia: tuning the system with microRNAs. *J Clin Invest* 2010; **120**: 3815–3817.
- Fasanaro P, D'Alessandra Y, Di Stefano V, Melchionna R, Romani S, Pompilio G *et al*. MicroRNA-210 modulates endothelial cell response to hypoxia and inhibits the receptor tyrosine kinase ligand Ephrin-A3. *J Biol Chem* 2008; **283**: 15878–15883.
- Giannakakis A, Sandaltzopoulos R, Greshock J, Liang S, Huang J, Hasegawa K *et al*. miR-210 links hypoxia with cell cycle regulation and is deleted in human epithelial ovarian cancer. *Cancer Biol Ther* 2008; **7**: 255–264.
- Crosby ME, Kulshreshtha R, Ivan M, Glazer PM. MicroRNA regulation of DNA repair gene expression in hypoxic stress. *Cancer Res* 2009; **69**: 1221–1229.
- Ghosh G, Subramanian IV, Adhikari N, Zhang X, Joshi HP, Basu D *et al*. Hypoxia-induced microRNA-424 expression in human endothelial cells regulates HIF- $\alpha$  isoforms and promotes angiogenesis. *J Clin Invest* 2010; **120**: 4141–4154.
- Berghmans T, Ameye L, Willems L, Paesmans M, Mascaux C, Lafitte JJ *et al*. Identification of microRNA-based signatures for response and survival for non-small cell lung cancer treated with cisplatin-vinorelbine. A ELCWP prospective study. *Lung Cancer* 2013; **82**: 340–345.



**Cell Death and Disease** is an open-access journal published by Nature Publishing Group. This work is licensed under a Creative Commons Attribution-NonCommercial-ShareAlike 3.0 Unported License. The images or other third party material in this article are included in the article's Creative Commons license, unless indicated otherwise in the credit line; if the material is not included under the Creative Commons license, users will need to obtain permission from the license holder to reproduce the material. To view a copy of this license, visit <http://creativecommons.org/licenses/by-nc-sa/3.0/>

Supplementary Information accompanies this paper on Cell Death and Disease website (<http://www.nature.com/cddis>)